Institute of Microwave
and Wireless Systems

Leibniz
Universität
Hannover

2015 European Microwave Conference (EuMC)

Design and investigation of meshed patch antennas for applications at 24 GHz

Q. H. Dao
R. Braun
B. Geck

Design and Investigation of Meshed Patch Antennas for Applications at 24 GHz

Q. H. Dao, R. Braun, B. Geck
Institut für Hochfrequenztechnik und Funksysteme
Leibniz Universität Hannover
Hannover, Germany
dao@hft.uni-hannover.de

Abstract—This contribution presents optically transparent microstrip patch antennas which are designed using meshed conductors. The influences on antenna performance of meshing both patch and ground plane are studied. Important geometrical parameters which have the main impact on the operating frequency and bandwidth are pointed out. The investigation shows that a necessity of reducing the patch size and/or enhancing the bandwidth can be accomplished by the meshing method. Furthermore, antenna structures with an optical transparency of roughly 90 % can have comparable properties as a conventional patch antenna. A prototype is fabricated and the simulated and measured results are discussed.

Keywords—*Meshed Patch Antennas; Meshed Ground Plane; Transparent Antennas, K-band*
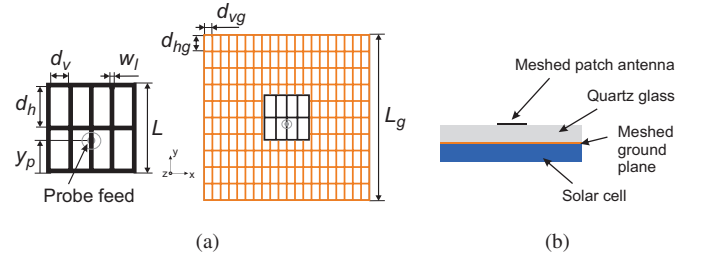
Fig. 1: (a) Geometry of a meshed patch (square) with 5 vertical lines, 3 horizontal lines ($N_v = 5$, $N_h = 3$) and meshed ground plane with 21 vertical lines and 11 horizontal lines ($N_{vg} = 21$, $N_{hg} = 11$). (b) One possible application of a meshed antenna on a solar cell (cross-section view)

I. INTRODUCTION

Nowadays, the Internet of Things (IoT) is an inherent part of the industry as well as of everyday life. There are many technologies offering the possibility to connect a device with a wireless communication system. A common technology that is widely used in this context is Radio Frequency Identification (RFID). In the field of production engineering such a system can improve the manufacturing processes as well as the component properties [1]. Another application of IoT are wireless sensor nodes (WSN) which are used to log the status of the component during its life cycle. In this scenario the WSN has to meet requirements such as small size and long life time. One possibility to extend the life cycle of the WSN can be carried out by an energy harvesting concept using a solar cell. To increase the integration level, the antenna can be placed above or even directly on the solar cell [2] [3]. In this case, a conductive material with high optical transparency is necessary [4]. However, the conductivity of transparent conducting oxides (TCOs) is only a fraction of conventional materials like copper whereas high antenna efficiency requires low electrical resistivity [5]. An alternative way to achieve optical transparency is meshing the surface of the antenna [6].

Usually meshed patch antennas have lower performance than their solid counterpart [7]. In order not to decrease the efficiency of the solar cell significantly the transparency of the meshed antenna should be as high as possible. Hence, there is a compromise to be found between optical transparency and antenna characteristics. Based on the investigation in the next section a meshed antenna operating at 24 GHz is designed in part III suitable to be integrated on a solar cell (cf. Fig. 1b).

II. ANTENNA DESIGN

The following investigations are carried out using a 3D full-wave simulator Ansys HFSS 2014. The geometrical dimensions of the square patch antenna are depicted in Fig. 1. A coaxial probe with an impedance of $Z = 50\,\Omega$ is used to feed the antenna. Quartz glass with a permittivity $\epsilon_r' = 3.96$ and a low loss angle $\tan\delta = 0.00016$ at 24 GHz is selected as carrier material. The thickness of the glass substrate is 0.2 mm and the square ground plane has a length of $L_g = 20$ mm.
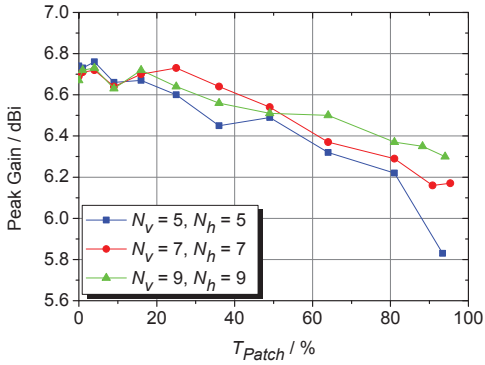
A. Meshed Patch

First of all, the radiating element of the microstrip patch antenna is meshed. For the definition of the grid the square patch is divided into strips with a line width w_l, while the length is kept constant ($L = 2.97$ mm). The variables N_v and N_h represent the number of vertical lines and horizontal lines, respectively. The distance d_v and d_h between the strips can be calculated by $(L - w_l)/(N_{v,h} - 1)$. The transparency T_{Patch} of the patch is defined by the ratio between the non-metal area and the total area of the solid structure.

First, the number of lines is fixed and the line width is varied in an interval from $w_l = L/N_{v,h}$ ($T_{Patch} = 0\,\%$) down to $w_l = 0.01$ mm. N_v and N_h are set to five, seven and nine, respectively. Fig. 2 depicts the influence on antenna properties caused by a variation of line width. The resonance frequency f_r and the resulting bandwidth (input reflection coefficient $|S_{11}| \leq$ - 10 dB) are shown in Fig. 2a. Its values (marked with squares) decrease with smaller line width while the transparency increases. Thus, the overall dimension of the meshed antenna can be reduced for a given operating frequency. The bandwidth reduces from 1.3 % to 0.3 %. It can be increased
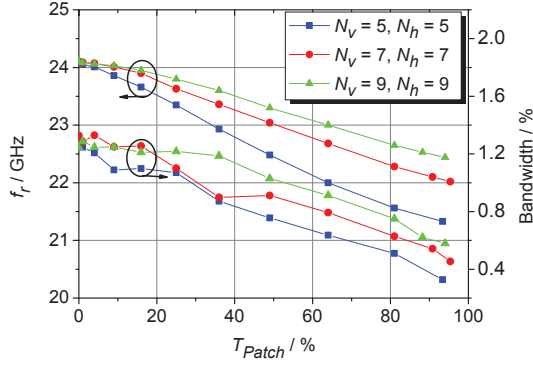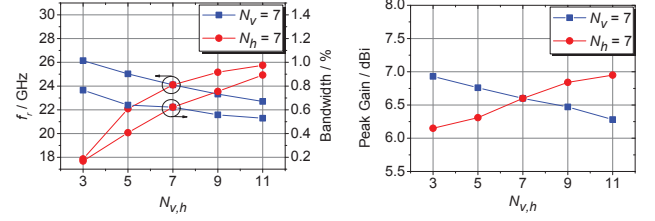
(a) Resonance frequency and bandwidth

(b) Peak Gain at f_r

Fig. 2: Effects of the line width (transparency) of the meshed patch on antenna performance for three configuration

(a) Resonance frequency and bandwidth

(b) Peak Gain at f_r

Fig. 3: Effects of the vertical and horizontal lines of the meshed patch on antenna performance for two cases ($N_v = 7$, $N_h = 7$)
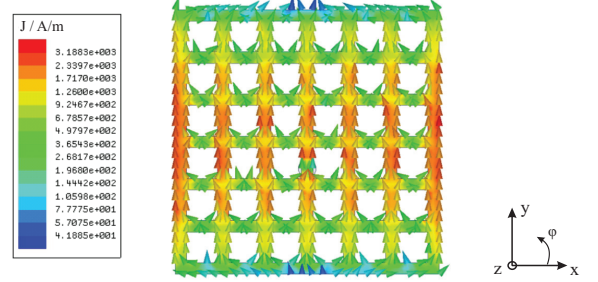

Fig. 4: Current density distribution of a meshed patch antenna ($T_{patch} = 50\%$) with a solid ground plane

applying additional lines at a fixed transparency (reduction of line width). The realized gain (peak gain) values are depicted in Fig. 2b. Meshing the patch decreases the peak gain values from about 6.7 dBi ($T_{Patch} = 0\%$) to 5.8 dBi. These characteristics are similar to [8].

So far, the number of vertical and horizontal strips are chosen to be equal. To achieve higher transparency the parameter N_v and N_h will now be varied independently. The starting configuration is set as follows: $L = 2.72$ mm, $w_l = 0.02$ mm, $N_v = 7$ and $N_h = 7$. This corresponds to a transparency of 90 %. The transparency for a combination of $N_v = 7$ and $N_h = 3$ or $N_h = 11$ is 93 % and 87 %, respectively. Fig. 3 shows the effects of the variation of vertical and horizontal lines on typical antenna characteristics. Hereby, the curves marked with squares represent the combination of seven vertical lines and variable number of horizontal lines, while the curves marked with circles depict the case of seven horizontal lines and different number of vertical lines. On the one hand, if the number of vertical lines is fixed a reduction of horizontal lines leads to higher resonance frequencies and bandwidths (marked with squares). On the other hand, a decrease of the number of vertical lines induces lower resonance frequencies and bandwidths. These trends can be observed at the curves of the realized gain, too. The results show, that the variation of the number of vertical lines has a higher impact on antenna performance whereas the main part of the current is on the vertical lines. These characteristics can be seen in Fig. 4. A

detailed analysis of the current distribution on the patch surface shows that the currents flow along both vertical and horizontal lines. Thus, it results in longer current paths (from the lower to the upper radiating edges) and the resonance frequency is lower compared to a conventional patch if the width of the mesh is decreased (for the same number of lines) or if the number of lines is reduced (for the same line width).

In order to obtain comparable simulation results the position y_p of the probe (cf. Fig. 1a) is varied in each configuration to achieve a good impedance matching ($|S_{11}| \leq -20$ dB). It is found that an increase of the transparency leads to a lower input resistance, which has to be compensated by different feed point positions [9].
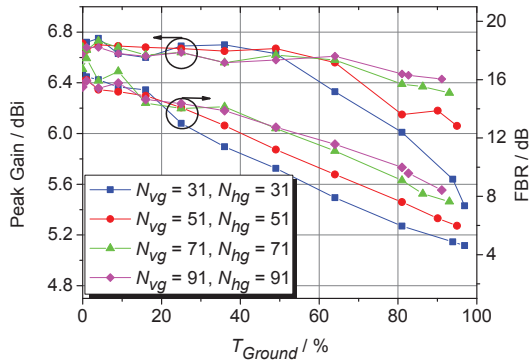
B. Meshed Ground Plane

Up to now, the meshed patch antenna is investigated with a solid ground plane. In order to obtain a transparent antenna structure the ground plane has to be meshed too. In the following study, the patch is modelled as solid ($T_{Patch} = 0\%$) in order to study the effects caused by meshing the ground plane on the antenna properties. In contrast to the analysis in the previous section the meshing of the ground plane has a minor influence on the input resistance. Thus, the location of the probe feed can be kept constant.

At first, the number of lines is fixed ($N_v = N_h = 31$) and the line width is varied from $w_l = L_g / N_{vg,hg}$ ($T_{Ground} = 0\%$) down to $w_l = 0.01$ mm. Fig. 5 shows the impact of the meshed ground plane on antenna characteristics by changing the transparency. As expected, the resonance frequency decreases with increasing spacing between the lines (cf. Fig. 5a). In contrast, the bandwidth behaves vice versa and it increases from 1.2 % to 3.5 %. If the ground plane consists of additional
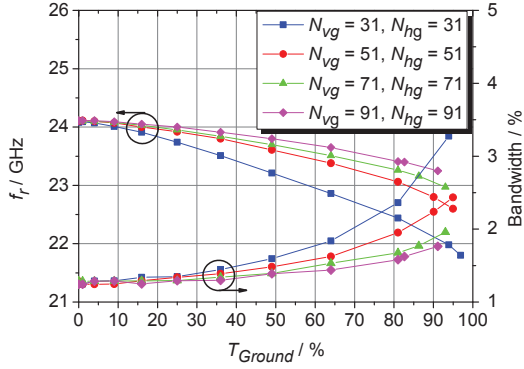
(a) Resonance frequency and bandwidth

(b) Peak gain and front-to-back ratio at f_r

Fig. 5: Effects of the line width (transparency) of the meshed ground plane on antenna performance for four configuration

Fig. 6: Radiation pattern of a patch antenna with solid and meshed ground plane ($w_l = 0.02\,\text{mm}$, $N_v g = N_h g = 51$, $d_{vg} = d_{vh} = 0.4\,\text{mm}$, $T_{Ground} = 90\,\%$)

(a) Resonance frequency and bandwidth

(b) Peak gain and front-to-back ratio at f_r

Fig. 7: Effects of the vertical and horizontal lines of the meshed ground planes on antenna performances for two cases ($w_l = 0.02\,\text{mm}$ and $N_{vg} = 51$, $N_{hg} = 51$)

number of lines (for a given transparency) these effects are less distinct. Meshing the ground plane gives the opportunity to enhance the bandwidth of patch antennas. The peak gain values decrease while refining the line width and this effect is more pronounced ($T_{Ground} \geq 80\,\%$) if the number of lines is reduced (cf. Fig. 5b). In consideration of the front-to-back ratio (FBR) it is obvious that these configurations radiate in the rear direction as well. The larger the distance $d_{vg,hg}$ between the grid, the higher is the back radiation. Fig. 6 depicts the radiation pattern of a patch antenna with both solid and meshed ground plane. It clarifies again that the meshed ground plane leads to higher radiation in the back direction than the solid counterpart. In addition, the meshing leads to a broader main lobe.

To obtain a higher transparency the number of vertical and horizontal lines can be varied independently as done in the previous section. The starting configuration is set as follows: $L = 2.8\,\text{mm}$, $w_l = 0.02\,\text{mm}$, $N_{vg} = 51$ and $N_{hg} = 51$. This leads to a transparency of $90\,\%$ and a spacing of $d_{vg} = d_{vh} = 0.4\,\text{mm}$. The transparency for a combination of $N_{vg} = 51$ and $N_{hg} = 31$ or $N_{hg} = 91$ is $92\,\%$ and $86\,\%$, respectively. Fig. 7 depicts the effects of different configurations on typical antenna characteristics. A closer examination of the resonance frequency, bandwidth, peak gain and FBR shows that a variation of the number of vertical lines has a higher impact on the antenna performance.
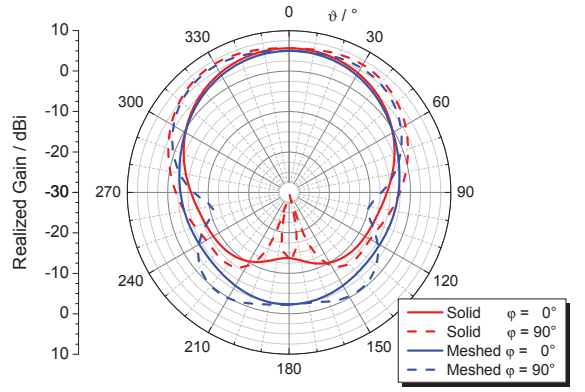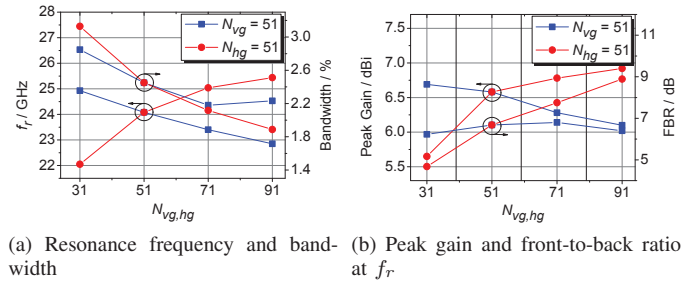
III. MESHED PATCH ANTENNA

The aim of the study is to design an antenna operating at the 24 GHz ISM band suitable for positioning on a commercial solar cell. For example a meshed antenna with a spacing of $d_v = d_h \approx 0.44\,\text{mm}$, $d_{vg} = d_{hg} \approx 0.4\,\text{mm}$ and a line width of $0.02\,\text{mm}$ corresponding to appr. $90\,\%$ transparency has a bandwidth of $1.76\,\%$ and a peak gain of $6.3\,\text{dBi}$. These values are determined by simulation.

Based on the investigation a meshed antenna is fabricated to evaluate the simulation results. To keep the manufacturing process as simple as possible the structure is designed on a RT/duroid 5880 substrate instead of the quartz glass. The measurement results depend highly on an accurate positioning of the probe feed. Thus, an inset feed is chosen to avoid this challenge. The front and the back side of the fabricated antenna are depicted in Fig. 8. The square ground plane has a dimension of $50 \times 50\,\text{mm}$. Due to limitations of the available etching process the line width w_l is chose to $0.15\,\text{mm}$. The meshed square patch consists of 7 vertical and horizontal lines and it has a length of $L = 3.8\,\text{mm}$ and a spacing of $d_v = d_h = 0.6\,\text{mm}$. The meshed ground plane composes of 75 vertical and horizontal strips and the grid has a gap of $d_{vg} = d_{hg} = 0.67\,\text{mm}$. Hence, the overall transparency is approximately $60\,\%$.

A. Measurement Results

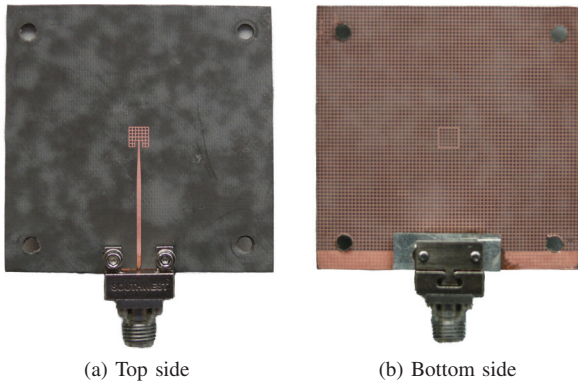The input reflection coefficient of the meshed antenna is measured with a network analyser. The calibration is carried

(a) Top side   (b) Bottom side

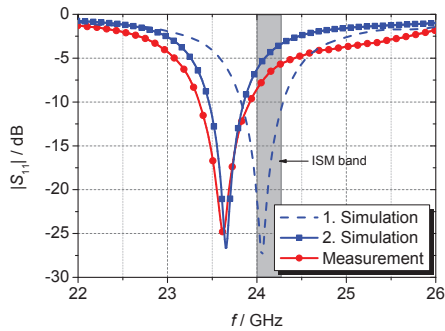Fig. 8: Pictures of the meshed patch antenna on RT/duroid 5880 substrate (transparency of metal mesh $\hat{=}$ approx. 60 %)

Fig. 9: Comparison between simulation and measurement of the fabricated prototype by means of the reflection coefficient

Fig. 10: Simulated and measured radiation pattern of the fabricated prototype

out by TRL method to de-embed the influence of the end launch connector. The simulated and measured curves of the reflection coefficient are shown in Fig. 9. The dashed curve represents the initial simulation result with a resonance frequency within the ISM band (1. simulation). Due to the inaccuracy of the fabrication process a small deviation of the line width is observed at the produced antenna. Hence, the structure is simulated again with the realized geometry parameters (2. simulation). The measurement result is depicted in the same figure to verify the simulation result. A good agreement can be obtained. The measured bandwidth is 2.4 % suitable for applications at the ISM band. Fig. 10 depicts the radiation pattern of the prototype. There is a slight deviation of 1.4 dB at $\vartheta = 0°$ (main direction, G_{meas} = 5.1 dBi). The back radiation can not be captured due to the measurement setup of the anechoic chamber. However, the radiation pattern can be verified by the measurement.

IV. CONCLUSION

This paper presents a study of the changes in antenna performance caused by meshing of the patch antenna as well as the ground plane. Applying the meshing method on the patch a lower resonance frequency can be achieved resulting in smaller dimensions for a given frequency. At the same time, the corresponding bandwidth and peak gain values are reduced. These effects are less dominant when the density of the grid gets higher at the same transparency (increasing the number of lines thus decreasing the line width). A reduction of vertical or horizontal lines leads to a higher optical transparency but
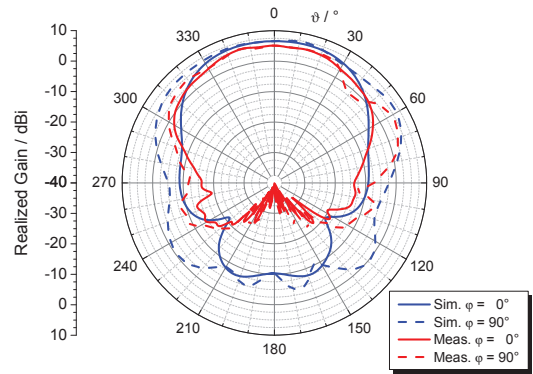
in this case influences on the current distribution must be taken into account. Decreasing the lines where the current density is high has a higher impact on resonance frequency and bandwidth. The peak gain decreases up to 0.9 dB and the radiation pattern is not significantly influenced by the grid. Based on the investigated geometry meshing the ground plane gives the possibility to enhance the bandwidth from 1.2 % (solid ground) to 3.5 %. Furthermore, the radiation pattern has a bit broader main lobe and the FBR decreases. Generally it can be said that the smaller the spacing between the lines is the higher is the antenna gain. However, there is a compromise to be found between highest optical transparency and optimal antenna properties. Based on the acquired knowledge a meshed antenna is fabricated. The comparison between measurement and simulation shows a good agreement.

REFERENCES

[1] J. Meyer, Q. H. Dao, and B. Geck, "24 GHz rfid communication system for product lifecycle applications," in *2nd International Conference on System-Integrated Intelligence: New Challenges for Product and Production Engineering (SysInt)*, 2014.

[2] M. Roo-Ons, S. Shynu, M. Ammann, S. McCormack, and B. Norton, "Transparent patch antenna on a-si thin-film glass solar module," *Electronics Letters*, vol. 47, no. 2, pp. 85–86, January 2011.

[3] T. Turpin and R. Baktur, "Meshed patch antennas integrated on solar cells," *Antennas and Wireless Propagation Letters, IEEE*, vol. 8, pp. 693–696, 2009.

[4] J. Saberin and C. Furse, "Challenges with optically transparent patch antennas," *Antennas and Propagation Magazine, IEEE*, vol. 54, no. 3, pp. 10–16, June 2012.

[5] T. Yasin, R. Baktur, and C. Furse, "A comparative study on two types of transparent patch antennas," in *General Assembly and Scientific Symposium, 2011 XXXth URSI*, Aug 2011, pp. 1–4.

[6] K. Ito and M. Wu, "See-through microstrip antennas constructed on a transparent substrate," in *Antennas and Propagation, 1991. ICAP 91., Seventh International Conference on (IEE)*, Apr 1991, pp. 133–136 vol.1.

[7] G. Clasen and R. Langley, "Meshed patch antennas," *Antennas and Propagation, IEEE Transactions on*, vol. 52, no. 6, pp. 1412–1416, June 2004.

[8] T. Turpin and R. Baktur, "See-through microstrip antennas and their optimization," in *International Union of Radio Science, XXIX General Assembly*, Aug. 2008.

[9] C. A. Balanis, *ANTENNA THEORY*, 3rd ed. John Wiley & Sons, 2005.